Whistler waves associated with weak interplanetary shocks

J. C. Ramírez Vélez,[1] X. Blanco-Cano,[2] E. Aguilar-Rodriguez,[3] C. T. Russell,[4] P. Kajdič,[2] L. K. Jian,[5,6] and J. G. Luhmann[7]

Received 31 January 2012; revised 6 September 2012; accepted 23 September 2012; published 6 November 2012.

[1] We analyze the properties of 98 weak interplanetary shocks measured by the dual STEREO spacecraft over approximately 3 years during the past solar minimum. We study the occurrence of whistler waves associated with these shocks, which on average are high beta shocks ($0.2 < \beta < 10$). We have compared the waves properties upstream and downstream of the shocks. In the upstream region the waves are mainly circularly polarized, and in most of the cases (~75%) they propagate almost parallel to the ambient magnetic field (<30°). In contrast, the propagation angle with respect to the shock normal varies in a broad range of values (20° to 90°), suggesting that they are not phase standing. We find that the whistler waves can extend up to 100,000 km in the upstream region but in most cases (88%) are contained in a distance within 30,000 km from the shock. This corresponds to a larger region with upstream whistlers associated with IP shocks than previously reported in the literature. The maximum amplitudes of the waves are observed next to the shock interface, and they decrease as the distance to the shock increases. In most cases the wave propagation direction becomes more aligned with the magnetic field as the distance to the shock increases. These two facts suggest that most of the waves in the upstream region are Landau damping as they move away from the shock. From the analysis we also conclude that it is likely that the generation mechanism of the upstream whistler waves is taking place at the shock interface. In the downstream region, the waves are irregularly polarized, and the fluctuations are very compressive; that is, the compressive component of the wave clearly dominates over the transverse one. The majority of waves in the downstream region (95%) propagate at oblique angles with respect to the ambient magnetic field (>60°). The wave propagation with respect to the shock-normal direction has no preferred direction and varies similarly to the upstream case. It is possible that downstream fluctuations are generated by ion relaxation as suggested in previous hybrid simulation shocks.

Citation: Ramírez Vélez, J. C., X. Blanco-Cano, E. Aguilar-Rodriguez, C. T. Russell, P. Kajdič, L. K. Jian, and J. G. Luhmann (2012), Whistler waves associated with weak interplanetary shocks, *J. Geophys. Res.*, *117*, A11103, doi:10.1029/2012JA017573.

1. Introduction

[2] Collisionless shocks are present in a variety of astrophysical plasma environments. In particular, a collisionless shock is permanently generated between the solar wind and the planetary magnetospheres. The intrinsic magnetic field of some of the planets, like the Earth, represents an obstacle for the solar wind in its trajectory through the interplanetary medium. A consequence of the encounter between the supersonic solar wind and the planetary magnetic field is that a bow shock is generated. The orientation of the magnetic field with respect to the shock-normal direction varies from quasi-parallel ($\theta_{BoN} < 45°$) to quasi-perpendicular ($\theta_{BoN} > 45°$) along the bow shock surface, where θ_{BoN} is the angle between the shock normal and the ambient magnetic field. Upstream of the quasi-parallel bow shock, an extended foreshock region is generated. A variety of phenomena are present in the foreshock; in particular, ion reflection can occur at the shock interface, and resulting ion beams can propagate back into the upstream region [e.g., *Asbridge et al.*,

[1]Instituto de Astronomía, Universidad Nacional Autónoma de México, Ensenada, Mexico.
[2]Instituto de Geofisica, Universidad Nacional Autónoma de México, México D.F., Mexico.

Corresponding author: J. C. Ramírez Vélez, Instituto de Astronomía/ Unidad Ensenada, Universidad Nacional Autónoma de México, Ensenada, México. (julio@astrosen.unam.mx)

0148-0227/12/2012JA017573

[3]Instituto de Geofisica/Unidad Michoacan, Universidad Nacional Autónoma de México, Morelia, Mexico.
[4]Institute of Geophysics and Planetary Physics, University of California, Los Angeles, California, USA.
[5]Department of Astronomy, University of Maryland, College Park, Maryland, USA.
[6]Heliophysics Science Division, NASA Goddard Space Flight Center, Greenbelt, Maryland, USA.
[7]Space Sciences Laboratory, University of California, Berkeley, California, USA.

1978; *Paschmann et al.*, 1981] generating low-frequency waves.

[3] Planetary bow shocks are not the only collisionless shocks in the solar system; there are also shocks generated when a fast stream of solar wind reaches a slow stream, producing an interplanetary (IP) corotating shock. Additionally, transient IP shocks can be generated by transient solar events like coronal mass ejections propagating in the solar wind. Most IP shock studies have concentrated on shock macrostructure, and little is known about their microstructure and the wave-particle phenomena around them. To know wave properties, it is important to learn about thermalization and acceleration processes at these shocks.

[4] At 1 AU, most stream interaction-driven IP shocks are weak, subcritical or marginally critical, so little or no ion reflection is likely to occur. In theory, laminar shocks can reach steady state through electrical resistivity alone and can provide dissipation through wave-particle interactions and through wave damping. Whistler waves can phase stand in the flow while the wave energy moves upstream and damps. Early theories [*Biskamp*, 1973] suggested that standing waves occurred downstream only when the shock became nearly perpendicular. However, recent works [*Balikhin et al.*, 2008; *Russell et al.*, 2009a] have shown that downstream compressive waves are observed often in laminar oblique shocks. Simulation work [*Ofman et al.*, 2009] explained the origin of these waves in terms of gyration of the downstream ions.

[5] *Fairfield* [1974] studied whistler wave properties produced in planetary high Mach number shocks, finding that the waves propagate obliquely (20°–40°) with respect to the magnetic field direction. Fairfield concluded that the analyzed waves follow a plasma dispersion relation for electron whistler waves and the typical wavelengths are associated with the thickness of the shock. *Hoppe et al.* [1981] studied the association of back-streaming ion fluxes and the whistler waves observed at the Earth's foreshock. They found that reflected ions are correlated with high-frequency (∼1 Hz) and low-amplitude whistler waves, while the diffuse ion distributions are associated with low-frequency (∼0.01 Hz) and large-amplitude waves. In a subsequent work, *Sentman et al.* [1983] studied the generation of 1 Hz whistler waves in the upstream Earth's foreshock. They conclude that the magnetic shock ramp could reflect electrons and the growth of the waves could be related to the Landau resonance of the waves with the reflected electron distributions with speeds above the electron thermal speed.

[6] *Tsurutani et al.* [1983] have studied the whistler wave properties associated with low Mach number interplanetary shocks. Analyzing data from the ISEE1 and ISEE2 magnetometers, they found two frequency regimes of waves, one at ∼0.05 Hz and the other, at 0.2–2 Hz. The latter, which is the high-frequency whistler precursor mode, is regularly situated upstream next to the shock interface, while the former is found much farther from the shock, upstream in the foreshock region. They have also found that whistler waves in the upstream region are, in general, not observed for shock geometries where $\theta_{BoN} > 65°$, being mainly present in oblique and quasi-parallel shocks. They found that the waves are propagating close to the magnetic field direction but without a preferred direction with respect to the shock normal (i.e., they conclude that the whistler waves are not phase standing). By comparing the thickness of the shock and the wavelength of the whistler precursors, the authors neglect that the shock is formed just as the last peak of the precursor wave. They suggested instead that the whistler waves with frequencies ∼1 Hz, which are adjacent to the shock, are generated at the shock interface by energetic electrons (10^2–10^3 eV) propagating upstream in some cases. They also argue that the waves with lower frequencies, ∼0.05 Hz, are likely to be produced locally by instabilities in the plasma situated far upstream.

[7] *Russell et al.* [1983] have also studied wave properties associated with IP shocks using the data from three ISEE magnetometers finding some consistent results with *Tsurutani et al.*'s [1983] study; namely, they also found two frequency regimes of waves. The first one at ∼1 Hz is the whistler precursor wave, situated adjacent to the shock. The whistler waves were found to propagate close to the magnetic field direction and were observed when the Mach number is between 1.3 and 1.7. The other wave regime, with lower frequencies, is associated with turbulent signatures farther upstream. The power spectrum of these waves is a broadband type in contrast to the (monochromatic) narrow peak spectrum of the high-frequency whistler waves.

[8] *Mellott and Greenstadt* [1984] have studied wave properties in a laminar (low β and low Mach number) shock regime in the Earth's bow shock. This regime is different than that of interplanetary shocks that have, in our investigated sample, low Mach number and high β. Mellott and Greenstadt also find the two previously mentioned wave frequency ranges. They identify the low-frequency waves (10^{-2} Hz) as the precursor standing waves which damp very fast as one moves away from the shock. They also show that when the shock does not exhibit a foot and overshoot as expected for supercritical Mach number shocks, the low-frequency precursor waves are part of the shock structure. For those laminar shocks the thickness of the shock corresponds to the precursor wavelengths. Concerning the high-frequency whistler mode at about 1 Hz in the spacecraft frame and comparing the wavelengths and amplitudes of both types of waves, they suggest that the high-frequency whistler waves are not a decay product of the precursor standing waves. They also found that high-frequency whistler waves propagate mainly parallel to the magnetic field.

[9] *Farris et al.* [1993] studied waves upstream of the subcritical and marginally critical Earth bow shocks for very low beta values (beta < 0.33) and found that the upstream region is permeated by both a phase standing low-frequency whistler wave very near the shock and higher-frequency whistler trains which can extend farther upstream.

[10] Recently, *Wilson et al.* [2009] presented a detailed analysis of the waves associated with five quasi-perpendicular IP shocks using data from the Wind spacecraft. In four weak IP shocks they found whistler waves that propagate quasi-parallel to the magnetic field but at large angles with respect to the shock-normal direction (30°–75°). In one strong IP shock, likely supercritical, a sequence of 12 shocklets with whistler waves was observed. Comparing the properties of the whistlers waves found in the four IP shocks without shocklets to those of the whistler waves found in the IP shock with shocklets, the authors found in the latter case that the whistlers propagate at more oblique angles with respect to the magnetic field and cover a broader range of values (10°–60°) than in the former case (20°–50°). Based on their data analysis and the

work of *Gary et al.* [1994], Wilson et al.'s study also concludes that the whistlers origin may be associated with an electron distribution unstable to the whistler heat flux and/or anisotropy instability. Finally, *Russell et al.* [2009b] have presented an analysis of the structure, formation and steepening of weak IP shocks. They have presented two cases of time series data from the STEREO mission in which a group of three IP shocks are registered in intervals of 1 h. Associated with these shocks are whistler waves with propagation direction oblique to the magnetic field direction.

[11] Numerical hybrid simulations (with fluid electrons and ions as particles) have also studied the properties and evolution of whistler waves upstream of shocks. For example, *Omidi et al.* [1990] found that in low Mach number quasi-parallel shocks, initially upstream whistler waves are phase standing waves with almost no ion heating contribution, with the last wave cycle forming the shock ramp. Nevertheless, this work also shows that due to the presence of reflected ion beams at the shock, at more evolved times, nonstanding waves are excited via the ion/ion beam instability. The *Omidi et al.* [1990] simulations are in one dimension, but *Scholer et al.* [1993] performed similar simulations in two dimensions. Scholer et al. found that initially the waves propagate along the normal direction but at later times and farther away in the upstream region they become more field aligned. More results and details about simulation works are given, for example, by *Scholer and Kucharek* [1999, and references therein].

[12] All the studies mentioned above, that form a nonexhaustive list, show that the whistler wave properties can vary depending on different shock and plasma parameters, as for example the Mach and beta numbers, the shock strength and orientation and the presence of beam particles propagating downstream or upstream from the shock. In this work we study the characteristics of the waves within frequencies 0.1–3 Hz associated with IP shocks observed by the twin STEREO spacecraft [*Kaiser et al.*, 2008; *Acuña et al.*, 2008]. We have used 32 and 8 Hz resolution magnetic field data (with respective Nyquist frequencies of 16 and 4 Hz) to analyze wave properties and occurrence. Figure 1 provides and overview of solar wind velocity from 2007 to 2009, showing when the studied shocks with associated waves were observed. Given that this period corresponds to a solar minimum, most of the IP shocks are expected to be due to the interaction of fast and slow plasma flows.

[13] In section 2, we present the criteria used to classify when an IP shock is subcritical or supercritical. In section 3, we discuss in detail the wave properties of two IP shocks that we use as case studies. In section 4 we present the wave analysis, and we compare the properties of the upstream whistler waves to those of the downstream waves. In section 5, we analyze some plasma and IP shock properties of the shocks with waves, and we compare these properties to those of IP shocks where no waves were registered. Finally, in section 6, we present our conclusions.

2. Supercritical and Subcritical Shocks

[14] In this section, we briefly describe how we determine when a shock is supercritical. Traditionally, shocks have been classified in terms of their magnetosonic Mach number (M_{ms}), the ratio between the shock speed and the magnetosonic speed, which measures shock strength. When Mach number is small, below a critical number [e.g., *Kennel et al.*, 1985], the shock is laminar and dissipation can occur via whistler waves. It is when a shock reaches the critical value that the downstream flow velocity equals the downstream sound velocity [*Coroniti*, 1970] and then most of the waves do not stay near the ramp long enough to affect shock transition (i.e., through wave-particle heating, acceleration, etc.). Alternatively, when the Mach number is above a certain critical number, the shock becomes supercritical requiring more dissipation than can be accomplished by electrical resistivity [e.g., *Leroy*, 1983; *Kennel et al.*, 1985].

[15] To determine whether the shock is supercritical and assuming a gamma value of $\gamma = 4/3$, we followed the study of *Edmiston and Kennel* [1984] to theoretically determine the first critical Mach value (M_c). We present our results in terms of the ratio M_{ms}/M_c instead of the Mach number value. Because all the shocks in our sample are weak, the classification of the events goes from subcritical to moderate supercritical shocks ($M_{ms}/M_c < 2.1$ but in 96% of cases $M_{ms}/M_c < 1.6$). In four IP shocks of our sample there is a data gap in the plasma moments so no β parameter can be evaluated, preventing the determination of the critical Mach number values. Thus, we have excluded those shocks from that part of the study.

3. Case Studies

[16] We referred to the event list reported by the STEREO team to identify the IP shocks (http://www-ssc.igpp.ucla.edu/forms/stereo/). In this list, a forward shock is considered if the solar wind speed, proton number density, proton temperature, and magnetic field all increase simultaneously. In a reverse shock, the solar wind speed increases while the rest of elements decrease simultaneously. The shock list provides the beta, B_{down}/B_{up}, Mach number and θ_{BoN} parameters. The Rankine-Hugoniot conditions and the magnetic coplanarity theorem are used to determine the plasma shock parameters. The β parameter is calculated through the ratio of the perpendicular plasma (ion plus electron) thermal pressure to the magnetic pressure, where a constant electron temperature of 130,000 K is assumed. Due to the lack of alpha particle data, we assume its number density is 4% of the proton one, and its temperature is 4 times of the proton temperature; more details are given in the data Web site (http://aten.igpp.ucla.edu/forms/stereo/PLASTIC_parameter_definition.html). We investigated the occurrence of the whistler waves associated with the 98 IP shocks reported by STEREO A and/or STEREO B during the almost first 3 years of operation of the mission, from January 2007 to October 2009. During these 34 months the Sun was in a minimum period of activity such that all the IP shocks were weak, with magnetosonic Mach number values in the range 1.1 to 2.2, except in one case where M_{ms} = 2.6, and were driven mostly by stream interactions.

[17] We find that monochromatic waves in the frequency range 0.1–3 Hz were observed upstream and/or downstream, next to the transition region in 55% of the total sample of shocks. The maximum amplitudes of the waves were observed just next to the shock interface, reaching maximum

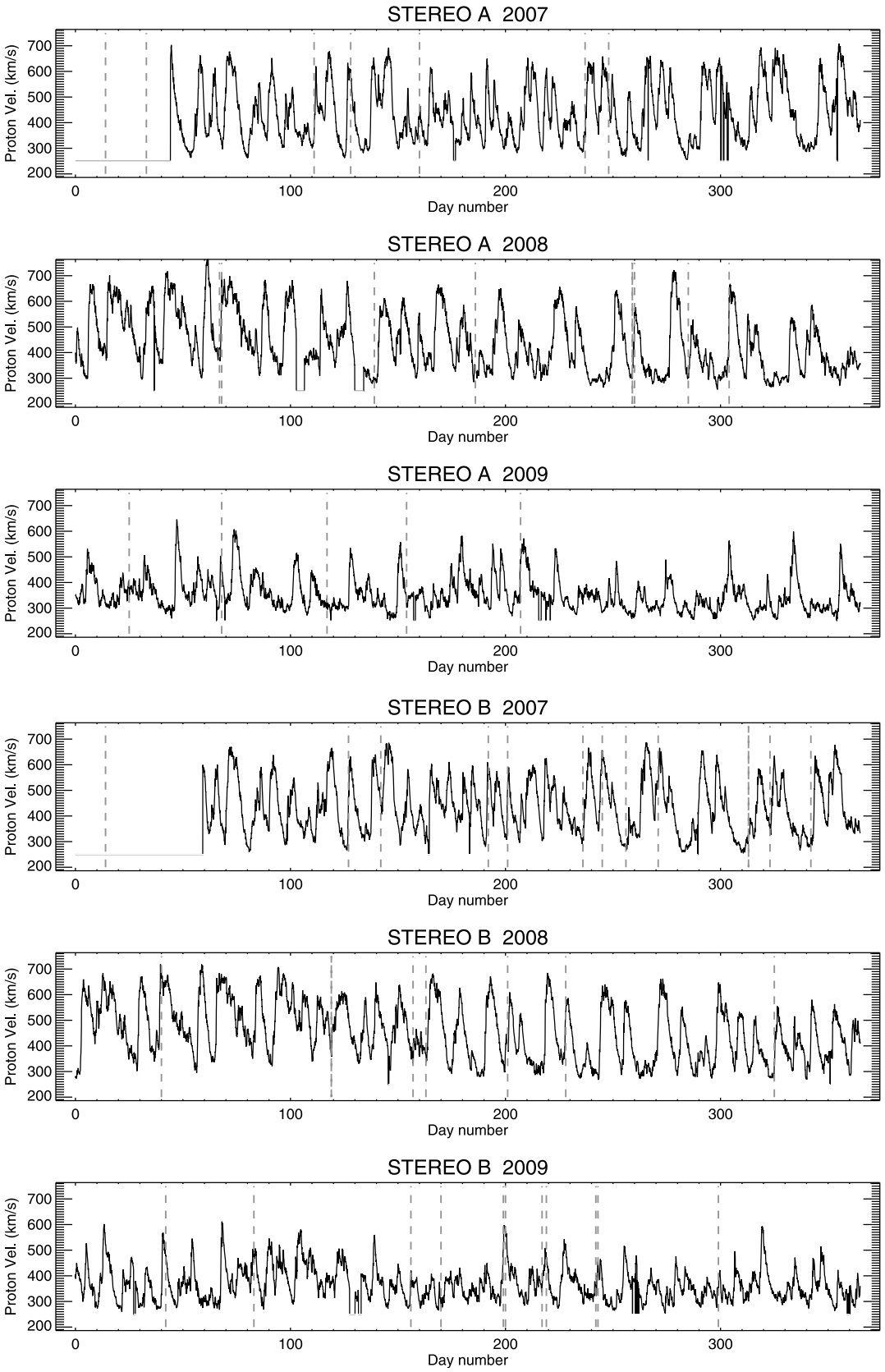

Figure 1. Plasma velocity registered by (first to third panels) STEREO A and (fourth to sixth panels) STEREO B during 2007–2009. No plasma data are available for early 2007. The shocks with associated waves considered in this work are indicated by the vertical lines. Most of the shocks are due to stream interaction.

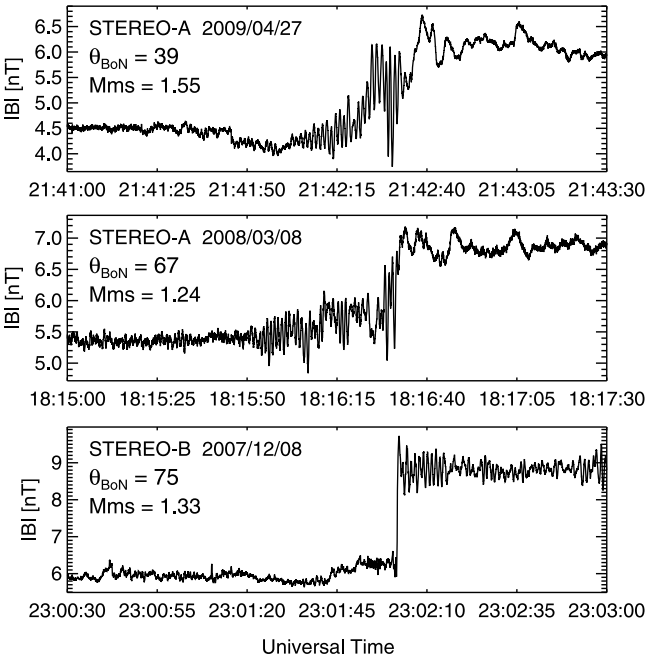

Figure 2. Magnetic field magnitude profiles for three shocks observed by STEREO with a time resolution of 32 Hz. (top) A quasi-parallel shock. (middle and bottom) Quasi-perpendicular examples.

normalized amplitude values of $\delta B/B_0 = 0.45$ and $\delta B/B_0 = 0.22$ upstream and downstream, respectively. The shock profiles and wave extensions vary depending on shock and plasma parameters.

[18] Figure 2 shows three examples of shocks observed by STEREO when operating on burst mode at 32 Hz, and Table 1 shows some shock parameters for each case. Figure 2 (top) corresponds to a quasi-parallel shock, where the transition from upstream to downstream has a gradual profile which is in contrast to the sharp profile of the quasi-perpendicular shock shown in Figure 2 (bottom). Note that on 27 April 2009, upstream whistler waves appear superposed on the gradual shock transition, and no whistler waves are observed downstream. Figure 2 (middle) shows an oblique shock with $\theta_{BoN} = 67°$. In this case the shock transition does not have a sharp gradient as expected for such an oblique shock, and whistler waves are found in an extended interval of the upstream region (see also Figure 3). The third example in Figure 2 (bottom) shows the typical sharp profile expected for a shock with a large θ_{BoN}, which in this case is 75°. Note that even when the Mach number is small, $M_{ms} = 1.3$, there is an overshoot. Note also that in this third example, large-amplitude waves are observed clearly in the downstream region but also during a very short interval, small-amplitude waves are observed in the upstream region.

[19] Figure 3 illustrates the whistler waves observed upstream of the oblique forward IP shock shown in Figure 2 (middle). The event was registered on 8 March 2008 by the STEREO A spacecraft at 18:16:32 UT. The shock was quasi-perpendicular with $\theta_{BoN} = 67°$, a ratio of plasma thermal pressure to magnetic pressure, $\beta = 1.7$, a ratio between the downstream and upstream field of $B_{down}/B_{up} = 1.3$, and a magnetosonic Mach number, $M_{ms} = 1.2$. Figure 3 (top) gives magnetic field components in shock-normal coordinates at a resolution of 32 Hz. The whistler waves in this case are present in the upstream region during an interval close to 2 min. As in all the cases, wave amplitudes are largest close to the shock. The minimum variance analysis (MVA) performed in the time interval from 18:14:10 to 18:16:00 UT, plotted in Figure 3 (bottom left), shows that the whistler waves are transverse circularly polarized and that their propagation is close to the ambient magnetic field direction ($\theta_{BoK} = 4°$). The ratio between the intermediate and minimum eigenvalues is high (Int/Min = 18) indicating that fluctuations are very planar. Figure 3 (bottom right) shows the power spectrum of the waves. The compressive power is obtained by applying the fast Fourier transform (FFT) to the magnetic field |B|, denoted as P_{Tot}, and the transverse power is defined as the difference of the power of the compressive part minus the addition of the power of the magnetic components: $|P_{Tot} - P_n - P_l - P_m|$, where P_n, P_l and P_m are three components of the magnetic field (see Figure 3 caption). In other words, the transverse power includes all the wave power that is not aligned to the field direction. The spectra of the whistler wave plotted in Figure 3 show that the transverse and compressional powers have both sharp peaks with maximum values close to ~1 Hz. The transverse power is dominant over the compressive one by 2 orders of magnitude.

[20] As can be seen in Figure 2 (middle), the downstream region of the shock on 8 March 2008 is permeated by some compressive low-frequency fluctuations, but MVA and wave power spectrum analysis showed no presence of whistler waves.

[21] Figure 4 shows the magnetic field data in the region just downstream on the 8 December 2007 shock, shown in Figure 2 (bottom). In this event the shock parameters are $\theta_{BoN} = 75°$, $\beta = 4.9$, $B_{down}/B_{up} = 1.4$, and $M_{ms} = 1.3$. Magnetic field components are given in the shock-normal coordinate system at a resolution of 32 Hz. During the first 10 s of the presented time interval we see very regular fluctuations of the B_l component and of the magnetic field magnitude. Nine waveforms are observed during this initial interval, indicating that their period was 1.1 s (frequency 0.9 Hz) in the spacecraft frame (see also Figure 4 (right)). The waves are highly compressive, which can be seen in the Fourier spectra in Figure 4 (right). However, the B_m and B_n components also fluctuate, although with smaller amplitudes. These fluctuations are also not as regular as the former. The relative phase difference between the fluctuations in B_l and B_m components is $\sim\pi/2$. Minimum variance analysis (not shown) indicates that the wave propagation direction is almost perpendicular to the magnetic field ($\theta_{BoK} = 89°$). After the initial 10 s the

Table 1. Shock Parameters Corresponding to the Three Shocks Shown in Figure 2

Parameter	STEREO A 2009/04/27	STEREO A 2008/03/08	STEREO B 2007/12/08
θ_{BoN}	39°	67°	75°
β	2.0	1.67	4.88
M_{ms}	1.55	1.24	1.33
M_c	1.28	1.70	1.17

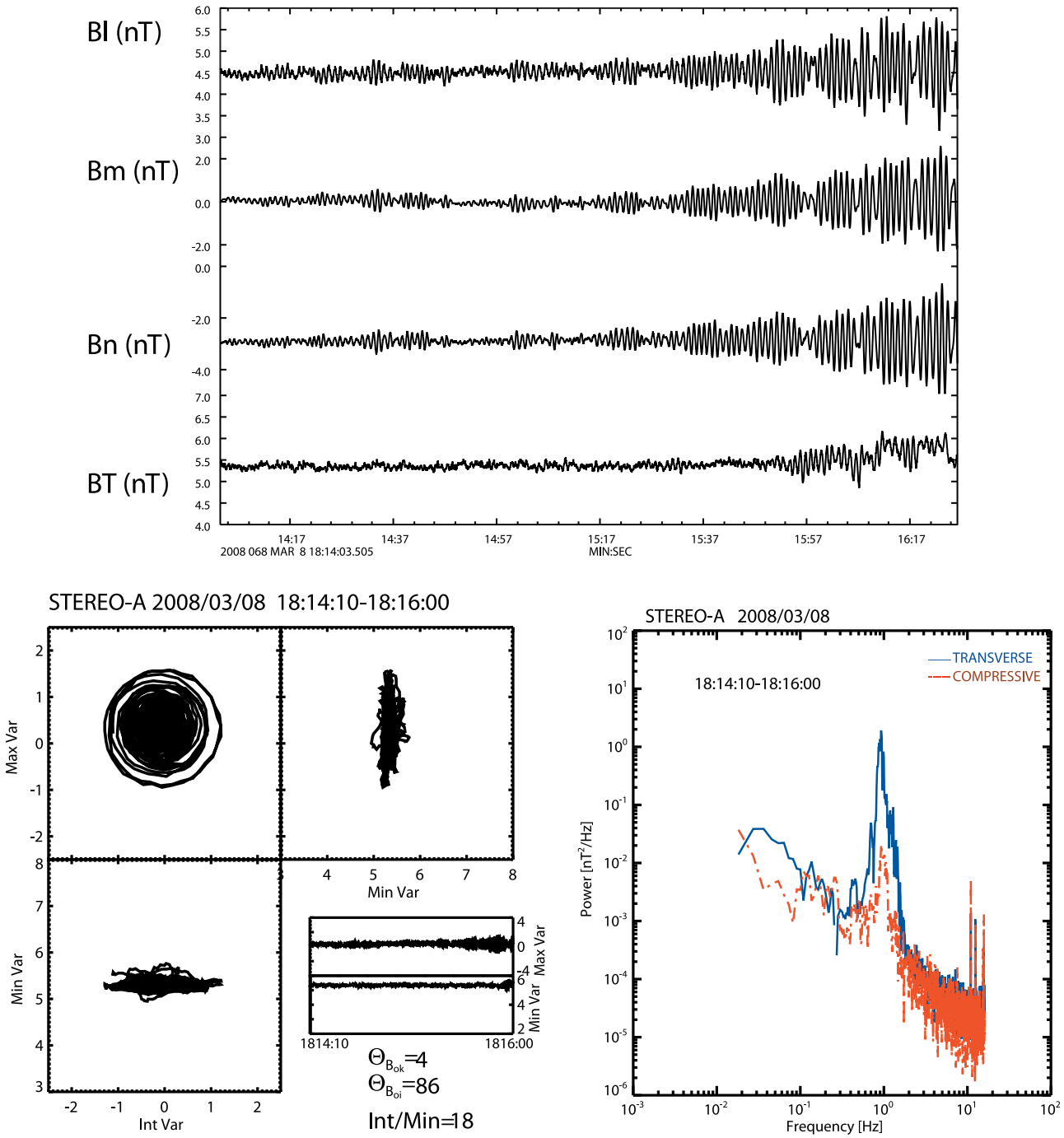

Figure 3. (top) Time series of the magnetic field data in shock-normal coordinates corresponding to the forward IP shock shown in Figure 2 (middle); n is along the shock-normal direction, l is on the shock plane parallel to the projection of the upstream average magnetic field, and m completes the right-handed system. Whistler waves are in the upstream region just before the shock interface. (bottom left and right) The minimum variance analysis and wave power spectrum correspond to the time interval 18:14:10–18:16:00 UT.

magnetic field fluctuations become highly damped and they are less regular.

[22] From the previous discussion we conclude that the analyzed downstream waves are highly elliptical, almost linearly polarized. They resemble the waves first described by *Balikhin et al.* [2008] that were observed downstream of the Venus bow shock, later found in the IP shocks driven by stream interaction [*Russell et al.*, 2009b] and explained in terms of kinetic relaxation by *Ofman et al.* [2009] using 1-D hybrid simulations.

[23] The waves shown in Figures 3 and 4 are examples that we used as case studies, but one of the goals of this work is to distinguish from our sample of 98 IP shocks consistent differences in the wave properties observed upstream or

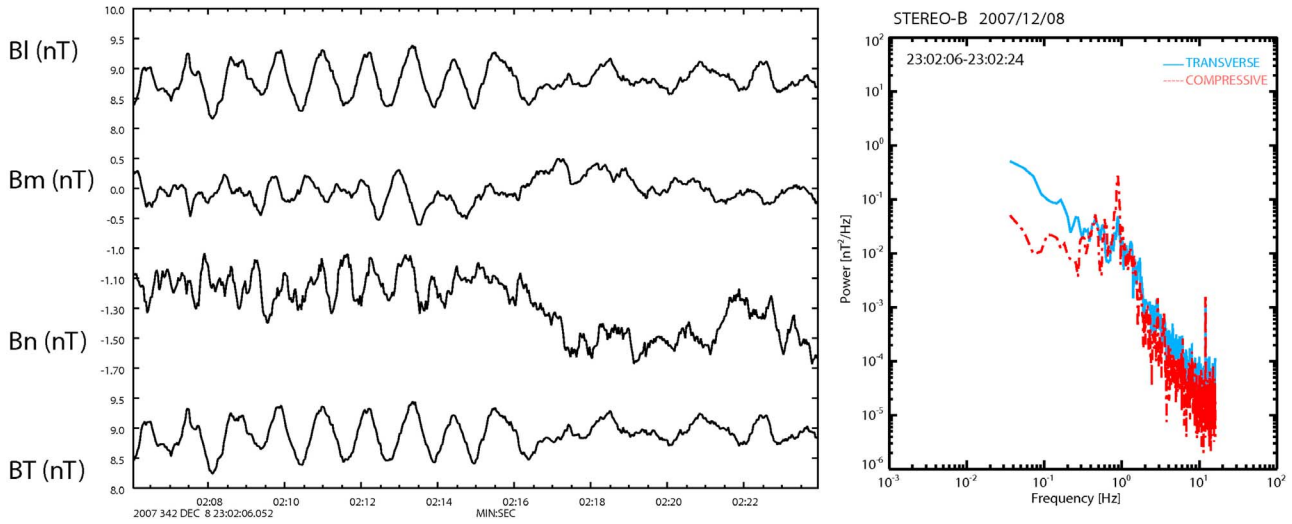

Figure 4. (left) Time series of the magnetic field data showing a small interval of the shock shown in Figure 2 (bottom). In this case, the observed waves are present in the downstream region. (right) The corresponding wave power spectrum.

downstream. We therefore present the characteristics of the waves at each of these two regions separately and compare the results. We have excluded all the cases in which the whistler waves properties were mixed with the properties of other types of waves (ion cyclotron, mirror mode, etc.). We have thus limited our selection to those cases where the waves with frequencies between $0.1 < f < 3$ Hz were clearly the dominant mode in the wave power spectra. We also study some of the plasma properties of the environment in which shocks with whistler waves are observed, as well as some of their associated shock properties, in order to investigate if there is any difference with the parameters of shocks where no whistler waves have been observed.

4. Wave Properties

[24] Whistler waves were observed upstream of the shocks in 28 cases, of the 98 cases of the total sample, while shocks with waves in the downstream region were found in 25 cases. In 3 cases of the shock sample, we have found waves in both regions of the shock, upstream and downstream. Minimum variance analysis shows that upstream whistler waves are mainly circularly polarized when the angle of propagation, with respect to the background magnetic field, is small ($\theta_{BoK} < 10°$) and they can become more elliptically polarized for the highest angles of propagation ($15° < \theta_{BoK} < 45°$). In contrast, downstream waves do not present any tendency of polarization, being either elliptical, linear or irregular polarized, among the whole range of angles of propagation ($14° < \theta_{BoK} < 90°$). Note, however, that no circularly polarized waves are present in the downstream region.

[25] Figure 5 shows (from top to bottom) normalized wave amplitudes ($\delta B/B_0$), the wave propagation angle with respect to the shock normal (θ_{KN}), the propagation angle with respect to the field direction (θ_{BoK}), and the wave frequency as a function of the shock strength (M_{ms}/M_c). Figures 5 (left) and 5 (right) show the properties of the waves observed upstream and downstream, respectively. The open circles correspond to quasi-parallel shocks ($\theta_{BoN} < 45°$), and the solid circles correspond to quasi-perpendicular shocks ($\theta_{BoN} > 45°$).

[26] The wave amplitudes showed in Figure 5 have been calculated as the mean value of all the wave cycles amplitudes. In both regions, upstream and downstream we observed an increase in normalized wave amplitude with increasing normalized Mach number. Also for both upstream and downstream regions, the increase in the wave amplitudes is considerably larger for the subcritical shocks than for supercritical shocks, and to evaluate it, we have performed a least squares fit for a function of the form $\delta B/B_0(X) \propto \exp\left(\frac{X}{A}\right)$, where $X = M_{ms}/M_c$ and A is the free parameter. We have additionally divided the shocks in function of the ratio of criticality. On one side we have fitted subcritical shocks where $M_{ms}/M_c \leq 0.9$, and on the other side we have fitted supercritical shocks where $M_{ms}/M_c \geq 1.1$. From the fitted functions we have found that for subcritical shocks the changes of wave amplitudes in the upstream and downstream regions are very similar ($A_{upstream} = 0.48$ and $A_{downstream} = 0.46$) while for supercritical shocks the increase of the amplitudes in the upstream region is slightly superior to the downstream region ($A_{upstream} = 3.7$ and $A_{downstream} = 4.4$). We finally remark that the maximum wave amplitudes are registered in the upstream region, with $0.07 < \delta B/B_0 < 0.45$ for waves upstream and $0.04 < \delta B/B_0 < 0.22$ for waves downstream.

[27] The θ_{KN} plots in Figure 5 show that the wave angles of propagation with respect to the shock normal cover a broad range of values, with θ_{KN} between 19° and 82° upstream and between 9° and 87° for downstream fluctuations. Our conclusion is that there is no clear tendency as the dispersion of the angle θ_{KN} is significant for waves in both regions, upstream and downstream.

[28] The θ_{BoK} plots in Figure 5 show the wave propagation angle with respect to the magnetic field direction. With the help of the MVA we also estimated the error in the

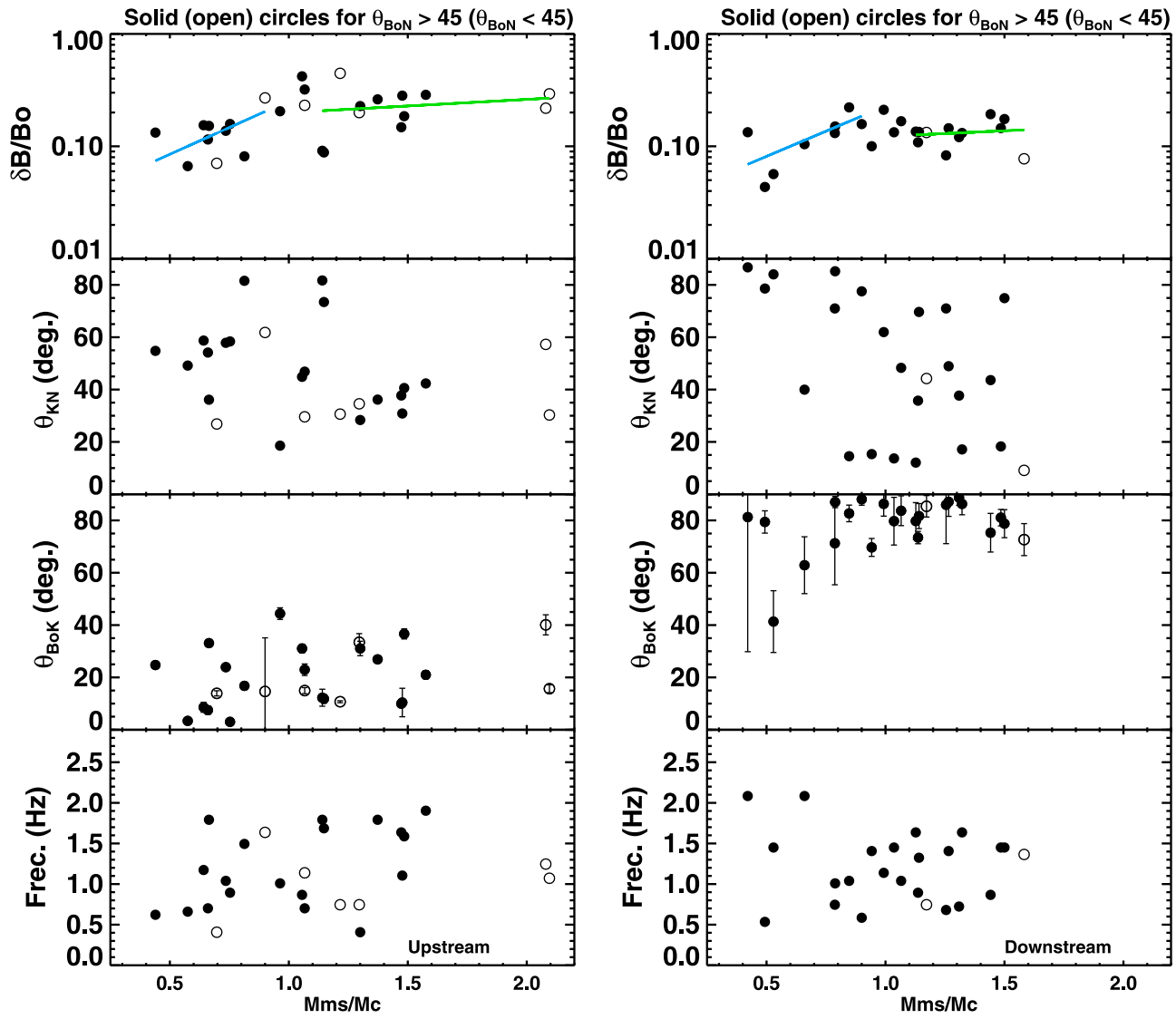

Figure 5. Wave properties as function of shock strength. From top to bottom, first panel is in a semilog scale and second to fourth panels are in a linear scale. (left) For waves in the upstream region (26 cases) and (right) for waves in the downstream region (28 cases). The solid symbols correspond to $\theta_{BoN} > 45°$, and the open symbols correspond to $\theta_{BoN} < 45°$.

determination of θ_{BoK}. As explained in the study of *Sonnerup and Scheible* [1998] for spacecraft data analysis, the error is given by

$$\Delta\theta_{BoK} = \sqrt{\frac{\lambda_3}{M-1}\frac{\lambda_2}{\lambda_2-\lambda_3}}, \quad (1)$$

where λ_2 and λ_3 are the intermediate and minimum eigenvalues, respectively, and M is the number of magnetic field vectors.

[29] In the upstream region, the waves propagate at $\theta_{BoK} < 30°$ in 73% of the events, in contrast to the downstream region where the waves propagate at $\theta_{BoK} > 60°$ in 95% of the cases. Note that waves in the downstream region tend to not be planar so the K direction determined with minimum variance analysis has more error than for the upstream cases.

[30] The values obtained for θ_{KN} and θ_{BoK} for the upstream whistler waves are consistent with the results of *Russell et al.* [1983] and *Tsurutani et al.* [1983]; that is, waves propagate at small angles with respect to the upstream magnetic field and show no order of propagation direction with respect to the shock normal. This suggests that these upstream whistlers waves are not phase standing fluctuations, which propagate along the shock normal.

[31] The wave frequencies are also given in Figure 5. We have found that the predominant wave frequencies in the spacecraft frame are contained in the range 0.6–1.5 Hz in both regions, upstream (in 62% of cases) and downstream (in 75% of cases). The lower frequencies are 0.4 and 0.5 Hz for waves in the upstream and downstream regions, respectively, while the respective higher wave frequencies are 1.9 and 2.1 Hz.

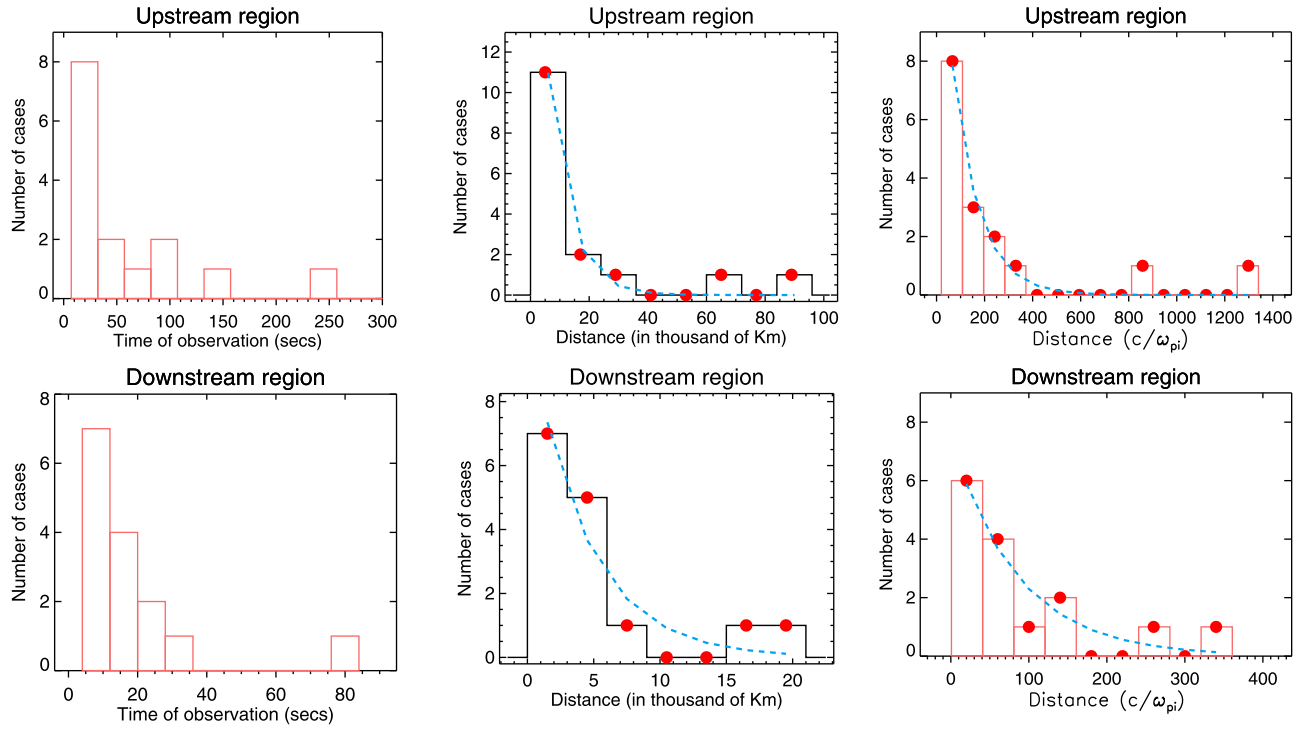

Figure 6. Histograms of the (left) duration and (middle and right) distance length of whistler waves. Figures 6 (top) and 6 (bottom) correspond to waves observed upstream and downstream, respectively. In Figures 6 (middle) and 6 (right), the dashed lines represent exponential fits; the obtained e-folding distances for the fitted functions are 13,500 km, or ~175 c/ω_{pi}, upstream and 5800 km, or ~100 c/ω_{pi}, downstream.

[32] From the analysis of the power spectrum for the upstream whistler waves, we found that fluctuations have a larger transverse component but they also exhibit a compressive component. Contrary, in the downstream whistler waves the compressive component clearly dominates over the transverse one.

[33] The extension of whistler waves upstream and downstream of the shocks is variable. To estimate the length that the waves can extend away from the shock interface, we have used the plasma velocity projected along the normal to the shock direction (in the spacecraft frame) and the time of observation of the waves through the spacecraft. In 23 IP shocks there is a gap in the plasma velocity data so we could only determine the extension of the waves in 16 cases for the upstream region and in 15 cases for the downstream region.

[34] Figure 6 (left) shows the histograms of the wave duration (time of observation), and Figures 6 (middle) and 6 (right) show the histograms of the extension of the waves projected along the shock-normal direction. Figure 6 (middle) is in units of kilometers, and Figure 6 (right) is in units of c/ω_{pi}, where c is the light speed and ω_{pi} is the proton plasma frequency. As can be seen in Figure 6 (top), most of the whistler waves in the upstream region (88%) are observed within 30,000 km (or 400 c/ω_{pi}) from the shock. However, in two cases of our sample the distance of the whistler waves is very large. From our data we cannot distinguish if in these two cases the waves propagate very far from the shock interface or if some local generation process is taking place. In any case, in a previous observational study, *Tsurutani et al.* [1983] found whistler waves up to ~12,000 km upstream from the IP shocks, which is lower almost by 1 order of magnitude than the larger regions we find permeated by whistler waves upstream from the shocks. In our sample, the largest distance with whistler waves upstream from the IP shock is 92,800 km (or 1300 c/ω_{pi}). Our results are in agreement with the distances at which whistler waves have been observed upstream of planetary bow shocks [*Russell*, 2007]. Finally, we have performed a fit of an exponential decay of the whistler extension, $d \propto \exp(-X/A)$. We have found that $A_{upstream}$, i.e., the upstream e-folding distance, is 13,500 km (or ~175 c/ω_{pi}).

[35] In the downstream region (Figure 6, bottom), the waves are limited to the neighborhood of the shock interface reaching maximum extensions of 18,200 km (or 350 c/ω_{pi}). The exponential fit of the decay of the whistler length ($d \propto \exp(-X/A)$) in this case is $A_{downstream}$ equal to 5800 km (or ~100 c/ω_{pi}).

[36] To finish the analysis of the wave properties, we have inspected the change in the wave propagation direction θ_{BoK} as the spacecraft is moving away from the shock interface. We selected only those cases where the extension of the wave trains was such that more than 20 wave periods were measured away from the shock.

[37] We have obtained the initial wave propagation direction for the first 10 wave periods next to the shock ($\theta_{BoK}^{initial}$), and we have then compared these values to the wave propagation direction for the last (the farthest) 10 wave periods from the shock (θ_{BoK}^{final}). We have also calculated the distance that separates the two regions from where $\theta_{BoK}^{initial}$ and θ_{BoK}^{final} were obtained.

[38] The change in the direction of propagation is defined as $\Delta\theta_{BoK} = \theta_{BoK}^{initial} - \theta_{BoK}^{final}$, such that positive (negative)

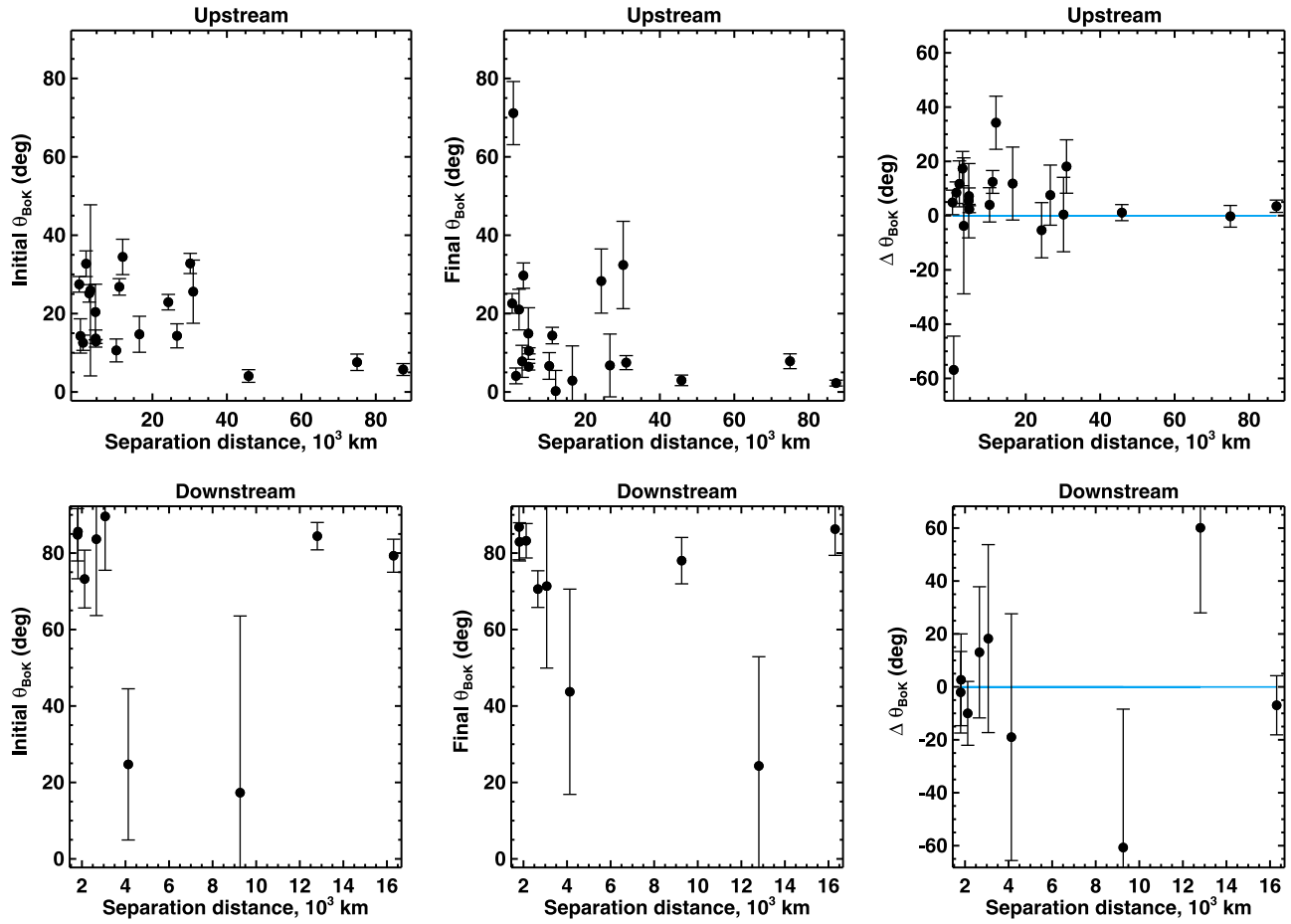

Figure 7. Variation of the wave propagation angle θ_{BoK} as function of distance to the shock; see the text for more details. The analysis results for the waves in the (top) upstream (20 cases) and (bottom) downstream (9 cases) regions.

values of $\Delta\theta_{BoK}$ indicate that the wave propagation directions are becoming more (less) field aligned.

[39] We find that for the waves in the upstream region (Figure 7, top), the initial propagation direction has a mean value of $\langle\theta_{BoK}^{initial}\rangle = 19°$; in 50% of the cases $\theta_{BoK}^{initial} < 20°$, and the maximum value of $\theta_{BoK}^{initial}$ is 35°. For the final propagation direction (Figure 7, top middle), the mean value is lower, with $\langle\theta_{BoK}^{final}\rangle = 15°$, and the number of the cases where $\theta_{BoK}^{final} < 20°$ increases to 70%. There is only one case for which the final propagation direction has increased to $\theta_{BoK}^{final} = 71°$. Inspection of this case shows no particular feature so extra analysis is needed to find an explanation for this singular behavior.

[40] The wave propagation variations $\Delta\theta_{BoK}$ (Figure 7, top right) were positive (i.e., wave propagations become more field aligned) in 16 cases and were negative in 4 cases.

[41] With the presented wave properties we conclude that in general, upstream waves become more field aligned with increasing distance to the shock. This result, combined with the fact that the wave amplitudes also decrease as the distance to the shock increases, suggests that the waves could be Landau damped in the upstream region with increasing distance to the shock.

[42] We do not find any clear tendency for the direction of propagation of waves in the downstream region (Figure 7, bottom). It is important to remember that given that the downstream waves are very compressive fluctuations, the determination of θ_{BoK} has more error than for the case of upstream waves. We find that the initial and final angles of propagation cover similar range values. Most of the waves propagate at quasi-perpendicular directions with respect to the field, but there are also few cases where the waves are propagating close to the field orientation. However, and in contrast to the upstream fluctuations, the waves in the downstream region can have very large changes in propagation direction from nearly perpendicular to nearly parallel and vice versa, reaching maximum values of $\Delta\theta_{BoK}$ of +60° and −60°.

[43] With the presented analysis of $\Delta\theta_{BoK}$ for downstream waves and comparing to the upstream case, we consider that a more detailed study, which is beyond of the scope of this work, is required to understand more clearly the differences between changes in propagation direction between upstream and downstream waves.

5. Shock Properties

[44] In order to determine possible differences between IP shocks with waves and IP shocks with no waves, we have compared some shock parameters and plasma properties for shocks with and without waves. Figure 8 compares the beta

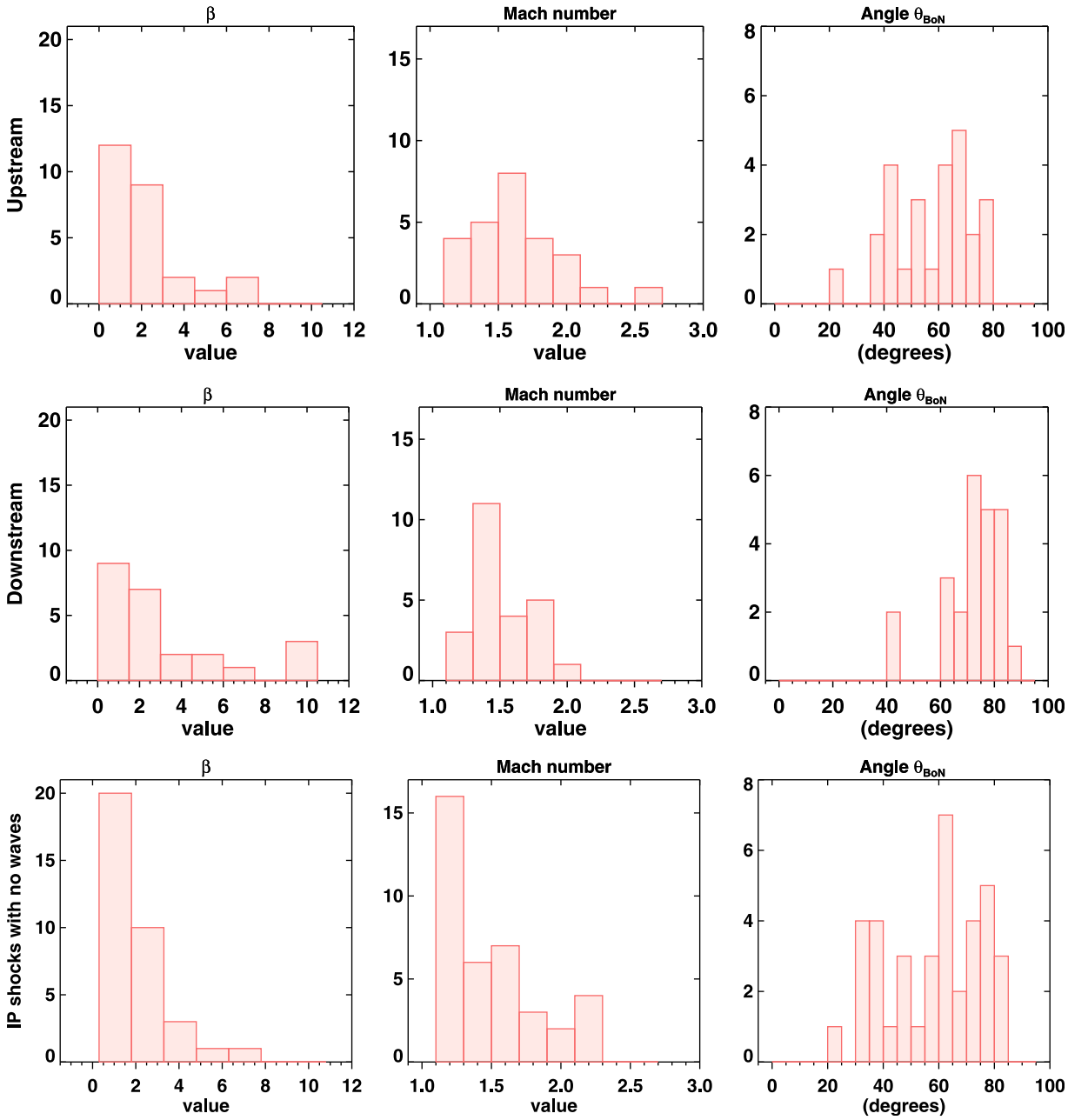

Figure 8. Histograms of the beta, Mach number and θ_{BoN} shock parameters in our sample. Shocks with whistler in the (top) upstream (26 cases) and (middle) downstream (24 cases) regions. (bottom) The case of shocks with no waves (38 cases).

parameter, the Mach number and the IP shock geometry for shocks where whistler waves were observed in the upstream region (Figure 8, top), for shocks with waves in the downstream region (Figure 8, middle), and for shocks where no waves were observed (Figure 8, bottom).

[45] Figure 8 (left) shows the histograms of the beta parameter (in the case of shocks without waves, Figure 8 (bottom left); in three cases beta was superior to 20, but we excluded them from Figure 8 for display purposes). We found that for shocks with waves in the upstream or downstream regions, the beta values are between 0.2 and 10, where in 78% of these cases the shocks have beta >1. Most of the shocks have moderate values of beta ($\beta < 5$): 92% for shocks with whistler waves in the upstream region, 75% for shocks with waves in the downstream region and 87% for shocks with no whistler waves. The maximum beta values are 7, 10 and 30, respectively.

[46] Figure 8 (middle) corresponds to the shock strengths, showing that in effect all the shocks in our sample have weak to moderate intensities. The maximum Mach numbers for shocks with waves in the upstream region, with waves in the downstream region and with no waves are 2.6, 2.0 and 2.2, respectively. We remark, however, that the three peaks of the Mach number distributions correspond all to low Mach number values.

[47] Figure 8 (right) corresponds to the shock geometry. In shocks with whistler waves in the upstream region the angles θ_{BoN} cover a broad range of values, $25 < \theta_{BoN} < 80°$, contrary to shocks with waves in the downstream region where the angle distribution is more concentrated in quasi-perpendicular geometries, $44 < \theta_{BoN} < 86°$. In shocks with no waves the angle distribution also covers a broad range of values, $21 < \theta_{BoN} < 82°$, but most of the shocks are quasi-perpendicular.

[48] Previous observational studies have pointed out that whistler waves are, in general, not generated for shocks with highly oblique geometry where $\theta_{BoN} > 75°$ [*Tsurutani et al.*, 1983; *Mellott and Greenstadt*, 1984; *Winterhalter and Kivelson*, 1988]. However, we do observe whistler waves in shocks with high θ_{BoN}. In our sample we observe upstream whistler waves for shock geometries nearly perpendicular ($\theta_{BoN} > 75°$) in 3 cases (which represents the ~10% of the upstream analyzed cases). The number of IP shocks with waves downstream where $\theta_{BoN} > 75°$ is 12, which corresponds to 50% of the downstream wave cases. Note that no whistler waves are found for nearly parallel geometries since no IP shocks in our data set had $\theta_{BoN} < 20°$.

[49] Our main result from the comparison shown above, between shocks with and without waves, is that there is no clear difference between the properties of shocks where waves are observed and those where no whistler waves are observed. In other words, no prediction of whistler occurrence can be established from the analysis of these plasma and shock properties.

6. Discussion and Conclusions

[50] The extended solar minimum has provided us a good opportunity to study the characteristics of IP shocks generated by stream interactions and their associated whistler fluctuations. Because these shocks are mainly generated by solar wind stream interaction and at 1 AU they have low Mach numbers, the sample observed by the STEREO mission during the years 2007–2009 is a good opportunity to study the behavior and transition of properties from "laminar" subcritical shocks to marginally supercritical shocks, with $M_{ms} \leq 2.6$.

[51] We have found that in the upstream region, the whistler waves are circularly polarized. In most of the cases (92%), their propagation direction is contained within an angle of 40° with respect to the magnetic field vector, their mean wave amplitudes increase exponentially with the Mach number and the wave angle of propagation with respect to the shock normal (θ_{KN}) covers a broad range of values, with θ_{KN} between ~20° and 90°. These properties of upstream whistlers suggest that they are not phase standing waves as predicted by laminar shock theory [*Biskamp*, 1973]. We have also found that the propagation direction θ_{BoK} for most of the upstream whistlers waves becomes more field aligned as the distance to the shock increases. In addition, given that the mean wave amplitudes also decrease with increasing distance to the shock, we then conclude that these two results suggest that it is likely the whistler waves suffer Landau damping in the upstream region.

[52] Most of the shocks observed by STEREO associated with stream interaction regions (SIRs) during the studied interval are not laminar. Even in those cases where M_{ms}/M_c is below 1, upstream waves propagate at smaller angles to the magnetic field and not along the shock normal. What is more, whistlers can extend almost up to 100,000 km upstream of the shock, which suggests that they are probably able to propagate away from the shock.

[53] Our results are in agreement with the results of *Tsurutani et al.* [1983] and *Russell et al.* [1983] and in contrast with the work of *Farris et al.* [1993] and *Fairfield and Feldman* [1975], who found upstream phase standing whistlers associated with the Earth's bow shock. The Mach numbers of the shocks in the samples of *Farris et al.* [1993] and *Fairfield and Feldman* [1975] were similar to the Mach numbers of the shocks observed by STEREO, but the plasma beta in their samples were very small, with values $\beta \leq 0.33$, while in our sample all cases have $\beta > 0.24$ and more than 75% have $\beta > 1$. The group velocity of the nonstanding whistler waves should be larger than, or comparable to, the upstream flow speed, such that the waves remain in the upstream region. At more intense shocks with $M_A > 3$ these waves should be convected back into the shock, causing its re-formation and downstream perturbations [*Krauss-Varban and Omidi*, 1993].

[54] Recently, nonstanding whistler waves have also been reported by *Wilson et al.* [2009], who studied wave association with electron distributions and explained that upstream whistlers are waves driven by electron instabilities. More work is needed to establish if whistlers in our sample are associated with back-streaming ions or electrons. Because our sample has many small Mach number shocks, it was expected that a laminar behavior was going to be observed in most of the cases; however, the beta values are not so small in our sample, and this can contribute to the enhancement of ion reflection because at high beta the kinetic effects become important. Finally, all the shocks we have analyzed have Mach numbers close to the transition from subcritical to supercritical shocks, and it is expected that in some of subcritical shocks, reflected ions could also be present [e.g., *Greenstadt and Mellott*, 1987], which could help to explain the wave properties we found in the upstream region of subcritical shocks.

[55] The properties of the waves downstream are very different from those upstream. We found that their polarization could be elliptical, linear or irregular, and in 95% of the events the wave propagation is contained in the range $\theta_{BoK} > 60°$. The change in the propagation of the downstream waves is in some cases irregular, and θ_{BoK} can pass from nearly aligned to the field to nearly perpendicular and vice versa. We remark, however, that because downstream waves are very compressive fluctuations, the determination of the angles of propagation shows a large error when calculated with minimum variance analysis. It is possible that some of the downstream waves are generated locally via ion relaxation as explained by *Ofman et al.* [2009] and that some are associated with waves generated at the shock.

[56] As the Sun becomes more active toward solar maximum, more interplanetary coronal mass ejections (ICMEs) are expected to drive shocks in the interplanetary medium. These shocks can be stronger than the ones associated with SIRs, so it will be of interest to study the shock transition properties as Mach number increases above $M_A > 3$ to test simulation predictions. Future works using hybrid simulations and full particle simulations will help to improve our understanding of the characteristics of IP shocks for different shock geometries and Mach numbers.

[57] **Acknowledgments.** J. C. Ramírez Vélez and E. Aguilar-Rodriguez thank PAPIIT project grant IN109112 and CONACyT project grant 101625. L. K. Jian is supported by the NASA STEREO program through grant NAS5-03131 administered by UC Berkeley. X. Blanco-Cano thanks CONACyT project grant 81154 and DGAPA grant 110511-3. P. Kajdič thanks CONACyT project grants 101625 and 81154 and PAPIT grant IN-110511-3.

[58] Philippa Browning thanks the reviewers for their assistance in evaluating this paper.

References

Acuña, M. H., D. Curtis, J. L. Scheifele, C. T. Russell, P. Schroeder, A. Szabo, and J. G. Luhmann (2008), The STEREO/IMPACT Magnetic Field Experiment, *Space Sci. Rev.*, *136*, 203–206, doi:10.1007/s11214-007-9259-2.

Asbridge, J. R., S. J. Bame, J. T. Gosling, G. Paschmann, and N. Sckopke (1978), Energetic plasma ions within the Earth's magnetosheath, *Geophys. Res. Lett.*, *5*(11), 953–955, doi:10.1029/GL005i011p00953.

Balikhin, M. A., T. L. Zhang, M. Gedalin, N. Y. Ganushkina, and S. A. Pope (2008), Venus Express observes a new type of shock with pure kinematic relaxation, *Geophys. Res. Lett.*, *35*, L01103, doi:10.1029/2007GL032495.

Biskamp, D. (1973), Collisionless shock waves in plasmas, *Nucl. Fusion*, *13*, 719–740.

Coroniti, F. V. (1970), Dissipation discontinuities in hydromagnetic shock waves, *J. Plasma Phys.*, *4*, 265–282.

Edmiston, J. P., and C. F. Kennel (1984), A parametric survey of the first critical Mach number for a fast MHD shock, *J. Plasma Phys.*, *32*, 429–441.

Fairfield, D. H. (1974), Whistler waves observed upstream from collisionless shocks, *J. Geophys. Res.*, *79*(10), 1368–1378, doi:10.1029/JA079i010p01368.

Fairfield, D. H., and W. C. Feldman (1975), Standing waves at low Mach number laminar bow shocks, *J. Geophys. Res.*, *80*(4), 515–522, doi:10.1029/JA080i004p00515.

Farris, M. H., C. T. Russell, and M. F. Thomsen (1993), Magnetic structure of the low beta, quasi-perpendicular shock, *J. Geophys. Res.*, *98*(A9), 15,285–15,294, doi:10.1029/93JA00958.

Gary, S. P., E. E. Scime, J. L. Phillips, and W. C. Feldman (1994), The whistler heat flux instability: Threshold conditions in the solar wind, *J. Geophys. Res.*, *99*(A12), 23,391–23,399, doi:10.1029/94JA02067.

Greenstadt, E. W., and M. M. Mellott (1987), Plasma wave evidence for reflected ions in front of subcritical shocks: ISEE 1 and 2 observations, *J. Geophys. Res.*, *92*(A5), 4730–4734, doi:10.1029/JA092iA05p04730.

Hoppe, M. M., C. T. Russell, L. A. Frank, T. E. Eastman, and E. W. Greenstadt (1981), Upstream hydromagnetic waves and their association with backstreaming ion populations: ISEE 1 and 2 observations, *J. Geophys. Res.*, *86*(A6), 4471–4492, doi:10.1029/JA086iA06p04471.

Kaiser, M. L., T. A. Kucera, J. M. Davila, O. C. St. Cyr, M. Guhathakurta, and E. Christian (2008), The STEREO Mission: An introduction, *Space Sci. Rev.*, *136*, 5–16, doi:10.1007/s11214-007-9277-0.

Krauss-Varban, D., and N. Omidi (1993), Propagation characteristics of waves upstream and downstream of quasi-parallel shocks, *Geophys. Res. Lett.*, *20*(11), 1007–1010, doi:10.1029/93GL01125.

Kennel, C. F., J. P. Edmiston, and T. Hada (1985), A quarter century of collisionless shock research, in *Collisionless Shocks in the Heliosphere: A Tutorial Review*, *Geophys. Monogr. Ser.*, vol. 34, edited by R. G. Stone and B. T. Tsurutani, pp. 1–36, AGU, Washington, D. C., doi:10.1029/GM034p0001.

Leroy, M. M. (1983), Structure of perpendicular shocks in collisionless plasma, *Phys. Fluids*, *26*, 2742–2753, doi:10.1063/1.864468.

Mellott, M. M., and E. W. Greenstadt (1984), The structure of oblique subcritical bow shocks: ISEE 1 and 2 observations, *J. Geophys. Res.*, *89*(A4), 2151–2161, doi:10.1029/JA089iA04p02151.

Ofman, L., M. Balikhin, C. T. Russell, and M. Gedalin (2009), Collisionless relaxation of ion distributions downstream of laminar quasi-perpendicular shocks, *J. Geophys. Res.*, *114*, A09106, doi:10.1029/2009JA014365.

Omidi, N., K. B. Quest, and D. Winske (1990), Low Mach number parallel and quasi-parallel shocks, *J. Geophys. Res.*, *95*(A12), 20,717–20,730, doi:10.1029/JA095iA12p20717.

Paschmann, G., N. Sckopke, I. Papamastorakis, J. R. Asbridge, S. J. Bame, and J. T. Gosling (1981), Characteristics of reflected and diffuse ions upstream from the Earth's bow shock, *J. Geophys. Res.*, *86*(A6), 4355–4364, doi:10.1029/JA086iA06p04355.

Russell, C. T. (2007), Upstream whistler-mode waves at planetary bow shocks: A brief review, *J. Atmos. Sol. Terr. Phys.*, *69*(14), 1739–1746.

Russell, C. T., E. J. Smith, B. T. Tsurutani, J. T. Gosling, and S. J. Bame (1983), Multiple spacecraft observations of interplanetary shocks: Characteristics of the upstream ULF turbulence, in *Solar Wind Five*, edited by M. Neugebauer, *NASA Conf. Publ.*, *CP-2280*, 385–400.

Russell, C. T., L. K. Jian, X. Blanco-Cano, and J. G. Luhmann (2009a), STEREO observations of upstream and downstream waves at low Mach number shocks, *Geophys. Res. Lett.*, *36*, L03106, doi:10.1029/2008GL036991.

Russell, C. T., L. K. Jian, X. Blanco Cano, J. G. Luhmann, and T. L. Zhang (2009b), STEREO observations of shock formation in the solar wind, *Geophys. Res. Lett.*, *36*, L02103, doi:10.1029/2008GL036337.

Scholer, M., and H. Kucharek (1999), Dissipation, ion injection, and acceleration in collisionless quasi-parallel shocks, *Astrophys. Space Sci.*, *264*, 527–543.

Scholer, M., M. Fujimoto, and H. Kucharek (1993), Two-dimensional simulations of supercritical quasi-parallel shocks: Upstream waves, downstream waves, and shock re-formation, *J. Geophys. Res.*, *98*(A11), 18,971–18,984, doi:10.1029/93JA01647.

Sentman, D. D., M. F. Thomsen, S. P. Gary, W. C. Feldman, and M. M. Hoppe (1983), The oblique whistler instability in the Earth's foreshock, *J. Geophys. Res.*, *88*(A3), 2048–2056, doi:10.1029/JA088iA03p02048.

Sonnerup, B. U. Ö., and M. Scheible (1998), Minimum and maximum variance, in *Analysis Methods for Multi-Spacecraft Data*, edited by G. Paschmann and P. W. Daly, pp. 185–220, Int. Space Sci. Inst., Bern.

Tsurutani, B. T., E. J. Smith, and D. E. Jones (1983), Waves observed upstream of interplanetary shocks, *J. Geophys. Res.*, *88*(A7), 5645–5656, doi:10.1029/JA088iA07p05645.

Wilson, L. B., III, C. A. Cattell, P. J. Kellogg, K. Goetz, K. Kersten, J. C. Kasper, A. Szabo, and K. Meziane (2009), Low-frequency whistler waves and shocklets observed at quasi-perpendicular interplanetary shocks, *J. Geophys. Res.*, *114*, A10106, doi:10.1029/2009JA014376.

Winterhalter, D., and M. G. Kivelson (1988), Observations of the Earth's bow shock under high Mach number/high plasma beta solar wind conditions, *Geophys. Res. Lett.*, *15*(10), 1161–1164, doi:10.1029/GL015i010p01161.